Fermi National Accelerator Laboratory

FERMILAB-Conf-95/190-E
CDF

B Production at CDF

P.T. Lukens
For the CDF Collaboration

Fermi National Accelerator Laboratory
P.O. Box 500, Batavia, Illinois 60510

July 1995

Published Proceedings for the *10th Topical Workshop on Proton-Antiproton Collider Physics*, Fermi National Accelerator Laboratory, Batavia, Illinois, May 9-13, 1995

Disclaimer

B Production at CDF

Patrick T. Lukens [1]

Fermilab, Batavia, IL 60510

Preliminary measurements of B meson cross sections, b quark cross sections, and $b-\overline{b}$ correlated cross sections are presented from the 1992-93 data obtained at CDF. A search for new states in the 75 pb^{-1} sample obtained through early 1995 yields no evidence for $B_c \rightarrow J/\psi - \pi$ or $\Lambda_b \rightarrow J/\psi - \Lambda^(1520)$.

Recent results on the measurement of b quark cross sections at The Collider Detector at Fermilab (CDF) have shown a consistant discrepancy with next-to-leading order QCD calculations (1). Preliminary results from the 1992-93 CDF data are now available, and represent a considerable improvement over earlier data, both in the sample size and quality. The larger sample size enables the measurement of the B meson differential cross section, an experimentally cleaner measurement than the inclusive lepton and J/ψ methods used previously. In addition, new measurements on $b-\overline{b}$ correlated cross sections are now made possible by the precision of the vertex detector used in the 1992-93 data. These cross section measurements and a search for new B hadrons will be presented here.

The CDF detector has been decribed in detail elsewhere (2). The b quark cross section measurements to be presented here are most dependent on the tracking and muon identification systems. Charge track reconstruction at CDF is performed in a three chamber system, which lies inside of a 1.4 T solenoidal field. The central drift chamber (CTC) reconstructs tracks in three dimensions, and is used for momentum measurement. A time projection chamber (VTX) is used to measure the primary vertex position along the direction of the beam. A silicon vertex detector (SVX) provides high precision measurement of charged particle impact parameters with respect to the primary vertex (3). This detector has acceptance over approximately 60% of the interaction region.

The analyses presented here make use of the muon identification system, which has an acceptance of approximately 75% for muons with $|\eta| < 1.0$. Both single muon and dimuon triggers are taken in a three level triggering system. At the first level, these triggers require the presence of muon chamber hits. The thickness of the hadron absorber requires that $p_t(\mu) > 1.4$ GeV/c. The second level of the trigger requires a coincidence between the muon chamber hits and high p_t track candidates found in the CTC fast track processor. Finally, the third level of the trigger path is a software reconstruction of tracks

[1] for the CDF collaboration

and muon chamber matching. Events with single muons above 7.5 GeV/c are kept, as well as dimuon candidates within 300 MeV/c^2 of the J/ψ mass.

B meson cross section measurements have been made with two different techniques; the complete reconstruction into hadronic final states, and partial reconstruction into semileptonic final states. Complete reconstruction gives the most accurate and model independent measurement, but the technique suffers from a small data sample, and is therefore limited to relatively low values of meson transverse momentum. The range of measurements is extended by the semileptonic technique, where the rate is higher. However, Monte Carlo techniques must be employed to estimate the meson momentum, since the neutrino and other decay products will carry some unmeasured momentum.

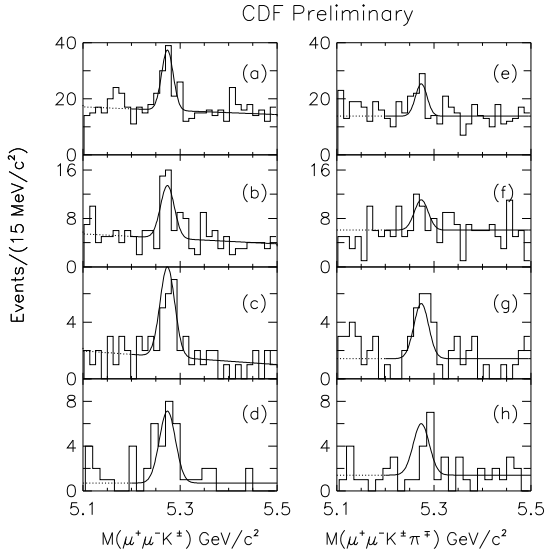

FIG. 1. a. The J/$\psi - K^{\pm}$ and J/$\psi - K^{*0}$ invariant mass distributions for transverse momentum ranges (a,e) 6-9 GeV/c, (b,f) 9-12 GeV/c, (c,g) 12-15 GeV/c, and (d,h) $>$ 15 GeV/c.

Exclusive reconstruction of B mesons is accomplished through the reconstruction of $B^+ \rightarrow J/\psi - K^+$ and $B^0 \rightarrow J/\psi - K^{*0}, K^{*0} \rightarrow K^+ - \pi^-$ (4), as well as their charge conjugates. Meson candidates are selected from dimuon triggers that with muon $p_t \geq 1.8$ GeV/c for one muon and $p_t \geq 2.8$ GeV/c for the other. The dimuon invariant mass is also required to fall within within 4σ of the accepted J/ψ mass (6). All oppositely charged, nonmuon tracks are considered as possible K^{*0} decay products, and $K\pi$ combinations within 50 MeV/c^2 are taken as K^{*0} candidates. For those situations where both mass assignments fall within this window, the assignment which yields the mass closest to the K^{*0} is taken. All tracks are required to have $p_t > 400$ MeV/c^2,

and all $K^{\pm}, K^{*0}$ are required to have $p_t > 1.25$ GeV/c. A constrained fit which requires the muon pair to form the accepted J/ψ mass (6) and all tracks to originate from a common vertex, is used to improve the momentum resolution of the final state. The invariant mass distributions for several values of transverse momentum are shown in Figure 1.

The number of B mesons in each range of p_t is found by fitting the invariant mass distributions. The background shape is estimated by the distribution of events that fail the χ^2 cut imposed on the vertex constrained fit. We have assumed that the B^+ and B^0 cross sections are indentical, so the two samples have been combined to give the best cross section measurement. After the neccesary corrections for acceptance and efficiency have been made, we find the values of the differential cross section listed in Table 1. Uncertainties listed are statistical and systematic, respectively.

TABLE 1. B meson differential cross section for $|y_B| < 1.0$

$< p_t >$ (GeV/c)	Cross Section (pb^{-1})
7.4	$596 \pm 103 \pm 106$
10.4	$116 \pm 24 \pm 21$
13.4	$55 \pm 10 \pm 10$
20.0	$7.2 \pm 1.4 \pm 1.8$

The B meson cross section at p_t of 18 GeV/c and above can be measured by partial reconstruction in semileptonic decay, $B \rightarrow \mu D \nu X$ (5). Single muon triggers are used in this analysis, and the remaining tracks are assigned kaon and pion masses in a search for $D^0 \rightarrow K^- \pi^+$, and the charge conjugate. We require the kaon and muon charges to be equal (ie., consistant with B decay), and the invariant mass of the $\mu - K - \pi$ system to be less than the B mass. Also, transverse momentum cuts are imposed which require both the kaon and pion to have $p_t > 1.5$, and at least one to have $p_t > 3.0$ GeV/c. The number of D^0's found is obtained by performing a Gaussian fit to the signal, along with a quadratic background. Events where the $K^- \pi^+ \pi^+$ and $K^- \pi^+$ mass difference is less than 153 MeV/c^2 are tagged as containing a D^{*+}, and provide a second measurement of B meson production. The $K\pi$ invariant mass distributions obtained in the inclusive muon data are shown in Figure 2.

The momentum of the $\mu - D$ system has been related to the momentum of the parent B meson by a Monte Carlo calculation. Events have been simulated by generating b quarks with $p_t > 15$ GeV/c using the DFLM parton distribution function and Peterson fragmentation with $\epsilon = 0.006$ (7). We have determined that the B meson momentum can be determined with a 15% resolution on an event by event basis. Again, we have assumed that the neutral and charged B meson cross sections are identical, and corrected the data for efficiencies and acceptances to yield a differential cross section. The results are shown in Table 2.

The summary of both complete and partial B meson differential cross sec-

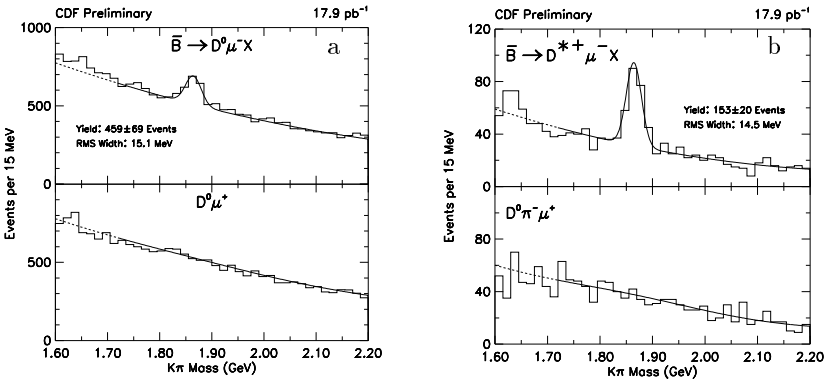

FIG. 2. a. The $K\pi$ invariant mass distribution when the K charge is the same and opposite the charge of the muon. b. Similar to a, but for events that contain a D^* tag.

TABLE 2. B meson differential cross section for $|y_B| < 1.0$

$< p_t >$ (GeV/c)	Cross Section (pb^{-1})	
	$B \to \mu D^0$	$B \to \mu D^*$
18-22	$12.1 \pm 2.8 \pm 2.0$	$10.8 \pm 2.6 \pm 1.9$
22-26	$5.7 \pm 1.3 \pm 1.0$	$5.9 \pm 1.2 \pm 1.1$
26-34	$2.0 \pm 0.5 \pm 0.3$	$1.2 \pm 0.3 \pm 0.2$

tion measurements is illustrated in Figure 3. Here, the results are plotted as a function of the B meson p_t, and are compared to a next-to-leading order QCD calculation (8) which uses the MRSD_0 structure function, a renormalization scale $\mu_0 = \sqrt{m_b^2 + p_t^2}$ a b quark mass of 4.75 GeV/c^2, and Peterson fragmentation (7). The theoretical uncertainties in the calculation have been estimated by varying the b quark mass between 4.5 and 5.0 GeV/c^2, the fragmentation parameter ϵ is varied from 0.004 to 0.008, and the renormalization scale varied from $\mu_0/2$ to $2 * \mu_0$. Current results clearly lie above the predicted cross section, although the shape of the data distribution is reasonably well described by the theory.

The largest systematic errors for both the full hadronic reconstruction and the partial semileptonic reconstruction of B mesons are the branching ratios into the final states we measure. These branching ratios have been measured by other experiments (6), and the cross section measurements we make depend on them. As more data become available, the p_t range of the full reconstruction will better overlap the range of the semileptonic technique, and this branching ratio uncertainty can be reduced.

The b quark cross section has been measured at still higher p_t by examining

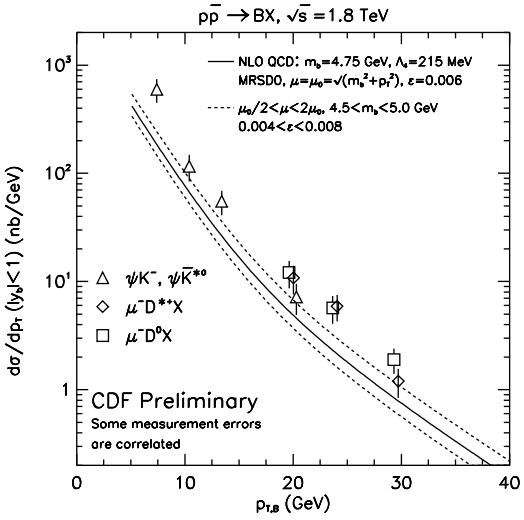

FIG. 3. B meson cross sections as a function of p_t(B). The solid curve is the prediction based on a next-to-leading order QCD calculation, and the dashed curves indicate the range of uncertainty in the calculation, based on modification of the parameters used.

the heavy quark content of jets obtained in an inclusive jet trigger. This analysis makes use of the precision track impact parameter measurements possible with the SVX. Jets with $E_t > 50$ GeV are passed through a tagging algorithm that identifies heavy flavor jets based on the presence of at least two non-primary tracks within the jet. An estimate of the proper flight distance $c\tau$ of the jet is then made by using these tracks.

This $c\tau$ measurement cannot be made without some corrections to the data, since the final state of the b quark is only partially measured. The HERWIG Monte Carlo (9) has been used to make this correction. Both $c - \overline{c}$ and $b - \overline{b}$ events were generated and simulated in the detector. These generated events then provided the correction factors needed to relate the measured track p_t to the initial quark momentum. This Monte Carlo sample also provided a predicted $c\tau$ distribution for each type of jet. These predictions, and the measured distribution, are shown in Figure 4. The data distribution was then fit to the sum of the three components to provide a total number of c and b quark jets.

The efficiency of the tagging algorithm has been measured with the Monte Carlo events, and found to be 5.3 $\pm$1.2% for c quark jets and 23 $\pm$ 5.3 % for b quark jets. The higher b quark efficiency is due to the longer lifetime and higher multiplicities of b hadrons. After corrections for trigger and acceptances, we find the fraction of charm jets in this sample

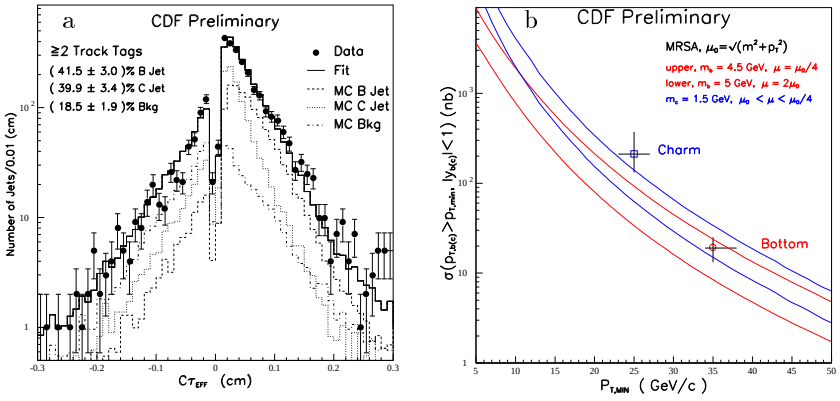

FIG. 4. a. The measured $c\tau$ distribution of inclusive jets, and the Monte Carlo predicted distribution for b, c, and direct jets. b. The measured cross section of b and c quark jets, compared to a next-to-leading order QCD calculation.

to be $8.83 \pm 0.75(stat)^{+2.25}_{-2.99}(syst)$, and the fraction of b jets to be $2.13 \pm 0.16(stat)^{+0.53}_{-0.56}(syst)$.

The cross sections for c and b quarks with $|y| < 1.0$ and $p_t > p_t^{min}$ has been measured with the inclusive jet sample as well. We define p_t^{min} as the p_t of the quark in a Monte Carlo distribution where 90% of the p_t distribution exceeds that value. In the Monte Carlo used here, we find that $p_t^{min} = 25.0 \pm 2$ GeV/c for c quarks and $p_t^{min} = 35.0^{+3}_{-1}$ GeV/c for b quarks. The measured cross sections are compared to a next-to-leading order calculation in Figure 4b. Similar to the case of B meson production, the measured quark cross sections are about a factor of two higher than predicted. The main systematic error in this technique is the uncertainty on the jet tagging efficiency.

Two different techniques have been used to measure $b - \overline{b}$ correlated cross sections, both of which are heavily dependent on the precision of the SVX to measure nonprimary tracks. The first method makes use of the dimuon trigger data, and performs a search for events where both b and $\overline{b}$ states decay into a final state which contains a muon. Events with two muons measured in the SVX, and with $p_t(\mu) > 3.0$ GeV/c for both muon candidates are used for this measurement. An explicit cut which requires that the dimuon invariant mass exceed 5 GeV/c^2 is used to reject sequential decays from a single b quark. The data is then divided into p_t bins, whiere $p_t(\mu_1) > 3.0$ GeV/c, and $p_t(\mu_2) > 3.0$, 5.0, and 7.0 GeV/c.

The lifetime of hadrons which contain a b quark will provide a number of decay muons with a large impact parameter with respect to the primary vertex. The muon impact parameter distribution for the data, and for Monte Carlo c and b quark decays are shown in Figure 5. The tails of these distributions at large impact parameter provide the discrimination power which enables the

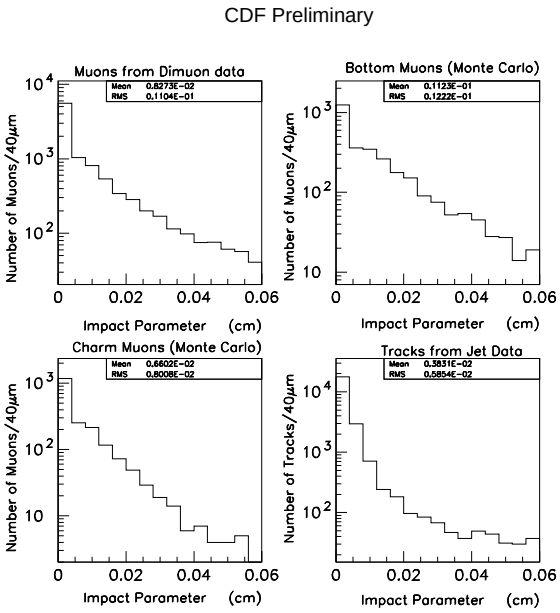

FIG. 5. The muon impact parameter distribution for dimuon data, Monte Carlo b and c quarks, and from inclusive jet data.

detection of the $b-\overline{b}$ events. The total number of $b-\overline{b}$ quark events has been obtained by fitting the data to a sum of the b, c, and background impact parameter distributions. Corrections are then made for efficiencies and acceptances to yield cross section measurements. The correlated cross section is then calculated for $p_t(b) \geq 6.5$ GeV/c, $|y_b| \leq 1.0$, $p_t(\overline{b}) \geq p_t^{min}$, $|y_{\overline{b}}| \leq 1.0$. These cross sections are plotted in Figure 6a, and compared to a next-to-leading order calculation of this process (10).

The correlations between muons has also been examined in this data, by studying the distribution of the opening angle between the muons in the transverse plane. The distribution found is shown in Figure 6b. The theoretical expectation (10) is also plotted here, both with and without the dimuon mass cut. As with the single b quark cross section measurements, the shape of distributions are well characterized by the theory, although the normalization appears too low.

The correlated $b-\overline{b}$ cross section has been measured at higher p_t by a technique that uses the single muon triggers, and evaluates jets in these events for their heavy flavor content (11). Events which are measured in the SVX have their jets evaluated for the probability that the jet originated from the

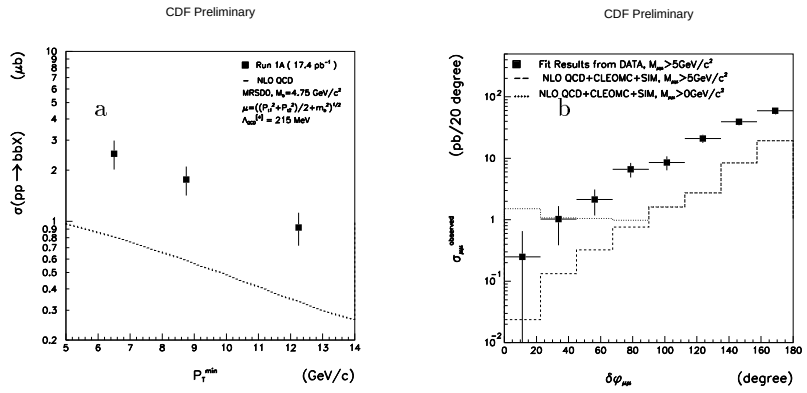

FIG. 6. a. The $b-\overline{b}$ cross section for $p_t(b) \geq 6.5$ GeV/c, $|y_b| \leq 1.0$, $p_t(\overline{b}) \geq p_t^{min}$, $|y_{\overline{b}}| \leq 1.0$. b. The transverse opening angle $\delta\phi_{\mu\mu}$ between the two muons, compared to the next-to leading order calculation.

primary vertex. This probability is based on the track impact parameters measured for the tracks in the jets. As in the inclusive jet measurement, the probability distribution seen in the data is fit to the sum of predicted distributions from b, c, and direct jets, to yield a measurement of the number of $b-\overline{b}$ events. This method yields measurements to $p_t(\mu) > 10$ GeV/c, and jet $E_t > 50$ GeV/c.

Two searches for new B hadrons have recently been made, which make use of 75 pb^{-1} of data, obtained through Feb., 1995. Both searches make use of the dimuon trigger sample, and the large, clean sample of J/ψ which are available. The first search is for the decay $B_c \rightarrow J/\psi - \pi$. This final state is similar to the more common $B^+ \rightarrow J/\psi - K^+$. The B^+ signal is used as a control sample, and the ratio of cross sections $\frac{\sigma * B(B_c \rightarrow J/\psi - \pi)}{\sigma * B(B^+ \rightarrow J/\psi - K^+)}$ is plotted for the mass range 6.1-6.4 GeV/c^2. Events are limited to the SVX acceptance, and this ratio is then calculated for various cuts on the assumed B_c lifetime, over the range 0-1.6 ps. At the 95% confidence level, we find $\frac{\sigma * B(B_c \rightarrow J/\psi - \pi)}{\sigma * B(B^+ \rightarrow J/\psi - K^+)} \leq 0.13$.

The second new particle search is for the $\Lambda_b \rightarrow J/\psi - \Lambda(1520)$, $\Lambda(1520) \rightarrow p - K$. This final state has good efficiency in the CDF detector, and has a control sample in the kinematicly similar $B^0 \rightarrow J/\psi - K^{*0}$. We measure the fraction of b quarks that fragment into Λ_b times the branching ratio into this fianl state to be $F(b \rightarrow \Lambda_b) * B(\Lambda_b \rightarrow J/\psi - \Lambda(1520)) < 2.8 * 10^{-4}$ at the 90% confidence level. The acceptance of the detector restricts this limit to $|\eta(\Lambda_b)| < 1.0$, and $p_t(\Lambda(1520)) > 2.0$ GeV/c.

The program of b quark production studies at CDF is varied, and able to address both the single b and correlated $b-\overline{b}$ cross sections over a wide range

of tranverse momentum. The technique of B meson reconstruction gives the cleanest, most direct momentum measurements, and provides differential cross section measurements. B meson cross sections have been measured from 6 to 34 GeV/c, and like the earlier work on integrated cross sections, these new measurements are higher than QCD calculations would predict. Future work will extend this technique to higher p_t, and allow a greater overlap between the hadronic decay and semileptonic decay results. This redundancy will reduce some of the systematic uncertainties in the measurements. Also, future work will include semileptonic decays in the electron channel, which will improve the statistical strength of the measurements. Higher p_t will be reached for integrated cross section measurements with the jet tagging techniques, and through the inclusive lepton spectra.

The addition of the precision track impact parameter measurements made by the SVX has provided CDF with the ability to measure correlated cross sections in a way not previously possible. This correlated cross section presents another test for QCD calculations. Future developments here will come with the wider range of p_t that a larger data set provides, as well as the eventual inclusion of electron decay channels to the analyses.

Finally, CDF provides a unique opportunity for the discovery of new B hadrons. The large B hadron event rates make rare process discovery possible, however the complexity of the hadron collider event presents a daunting challenge for finding the signals. No evidence has been seen for B_c or Λ_b in CDF data to date, but the addition of more data and development of new techniques may turn up these or other states in the future. Clearly, the future of B production work at CDF is a promising one, and should contribute significantly to our understanding of the b quark system.

REFERENCES

1. CDF Collaboration, F. Abe, *et. al.*, Phys. Rev. Lett. **71**, 2396 (1993).
2. CDF Collaboration, F. Abe, *et. al.*, Nucl. Instrum. Methods Phys. Res., Sect. A **271**, 387 (1988).
3. D. Amidei, *et. al.*, Nucl. Instrum. Methods Phys. Res., Sect. A **350**, 73 (1994).
4. Fermilab-Pub-95/48-E, submitted to Phys. Rev. Lett.
5. CDF Collaboration, T. LeCompte, ICHEP94.GLS0092, Fermilab-Conf-94/134-E
6. Particle Data Group, Phys. Rev. D, **45** (1992)
7. C. Peterson, *et. al.* Phys. Rev. D **27**, 105 (1983)
8. P.Dawson, *et. al.* Nucl. Phys. **B327**,49 (1988)
9. G. Marchesini and B.R.Webber, Nucl. Phys. **B310**, 461 (1988)
10. M. Mangano, *et. al.* Nucl. Phys. **b373** (1992)
11. CDF Collaboration, P. Derwent, ICHEP94 REF.GLS0122, Fermilab-Conf-94/129-E